

MRS DISTINGUISHED INVITED SPEAKER



From phase-change materials to thermoelectrics: The role of metavalent bonding

Yuan Yu^{1,a)}, Matthias Wuttig^{1,2,a)}

- ¹Institute of Physics (IA), RWTH Aachen University, 52074 Aachen, Germany
- ²Peter Grünberg Institute JARA-Institute Energy Efficient Information Technology (PGI-10), Wilhelm-Johnen-Straße, 52428 Jülich, Germany
- a) Address all correspondence to these authors. e-mails: yu@physik.rwth-aachen.de; wuttig@physik.rwth-aachen.de

Received: 22 April 2025; accepted: 27 May 2025; published online: 6 June 2025

Excellent phase-change memory materials and thermoelectrics are often found in chalcogenide compounds, in which they share a unique portfolio of properties. Quantum-chemical calculations indicate that these solids are characterized by the sharing of about one electron and a small number of electron transfers. In addition, atom probe tomography reveals an abnormal bond-breaking behavior. All of these factors indicate an unconventional bonding mechanism that differs from classical covalent, ionic, and metallic bonding, termed metavalent bonding. The adaptation of this bonding mechanism holds great potential for the development of phase-change and thermoelectric materials. For example, non-Zachariasen glasses have been identified for optoelectronic applications, where the crystallization rate can be tuned by changing the degree of electron sharing. Thermoelectric performance can also be significantly improved by forming metavalent bonds. Therefore, metavalent bonding offers a high degree of predictive power in tailoring properties for phase-change and thermoelectric applications.

Introduction

Chalcogenide compounds show promise in phase-change data storage and thermoelectric energy conversion. In phase-change materials (PCMs), the binary data "0" and "1" can be written and erased by rapidly switching the material between amorphous and crystalline states, as illustrated in Fig. 1(A) [1]. In thermoelectric materials, the directional movement of charge carriers (i.e., electrons and holes) driven either by a temperature gradient or a current can generate electricity or pump heat, respectively, as shown in Fig. 1(B) [2].

These two functionalities of chalcogenides have distinctively different property requirements. Specifically, PCMs require a fast phase transition between amorphous and crystalline states to improve the data read/write speed, a large optical/electrical contrast between these two states to warrant low data noise, and long thermal stability of the amorphous state to ensure data retention for at least a decade [3]. In contrast, thermoelectric materials require a large Seebeck coefficient (S) to create enough thermal power, a high electrical conductivity (σ) to minimize the internal resistance, and low thermal conductivity (σ) to maintain the temperature difference, as summarized in the dimensionless figure-of-merit, $zT = S^2 \sigma T/\kappa$, where T is the absolute

temperature [4]. Although the two application scenarios require distinctive yet different material properties, they often employ very similar compositions. For example, typical PCMs are found along the GeTe-Sb₂Te₃ tie line such as Ge₂Sb₂Te₅, or in the doped Sb₂Te alloys, or close to the Ag₅In₅Sb₆₀Te₃₀ (AIST) [5]. Similarly, outstanding thermoelectric performance is observed in compounds such as GeTe [6], (Bi, Sb)₂Te₃, [7] PbTe [8], and AgSbTe₂ [9]. It is striking that a similar group of materials can exhibit such diverse applications.

It is well known that the properties of solids such as the electronic band structures and phonon dispersions depend on the arrangement of the constituent atoms, i.e., the atomic structures. Moreover, the characteristic arrangement of atoms is determined by the chemical bonding mechanism present [10]. Therefore, understanding the bonding mechanisms of materials could reveal the origin of the similarity in stoichiometry between PCMs and thermoelectrics, which in turn helps in the design of these materials.

In this mini-review, we unravel the bonding origin of PCMs and thermoelectrics. We also discuss several bonding indicators and the behavior of bond rupture under high-field evaporation of atoms. Finally, we present the design of PCMs and



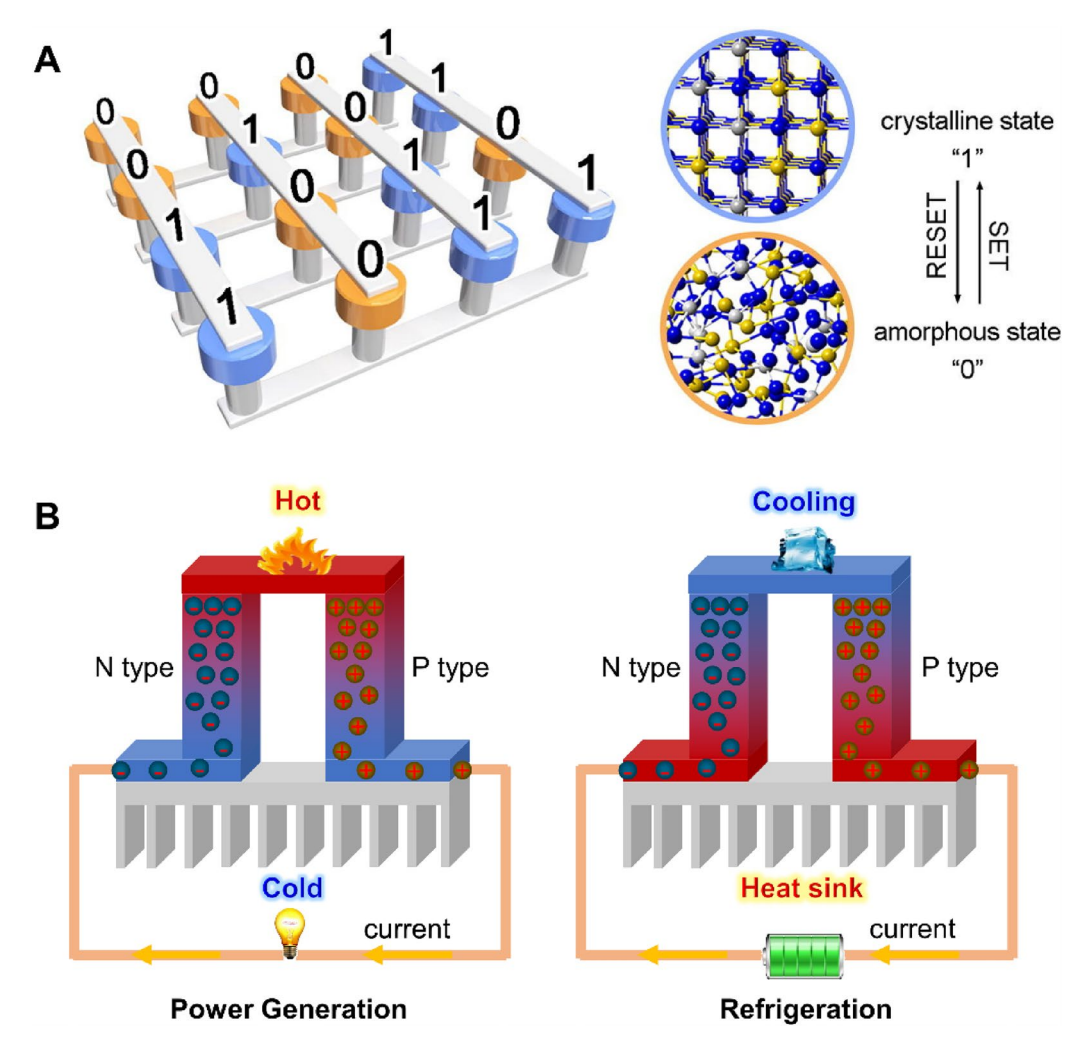


Figure 1: Schematic of phase-change materials (PCMs) and thermoelectric materials. (A) The crystalline and amorphous states of PCMs are used to store binary "1" and "0," respectively. These two states can be switched reversibly by either applying a laser or a voltage pulse. Adapted from Ref. 1. (B) Thermoelectric power generation by harvesting heat based on the Seebeck effect and solid-state refrigeration by applying a direct current based on the Peltier effect.

thermoelectrics based on the understanding and tailoring of chemical bonds.

Metavalent bonding

Chemical bonds are formed by the interactions of the outershell electrons of atoms. The behavior of these electrons can be quantitatively described by solving the Schrödinger equation. Figure 2 presents a bonding map spanned by the number of electrons transferred normalized to the oxidation state of atoms (ET) and the number of electrons shared (ES) between adjacent atoms [11–13]. These values have been derived from the quantum theory of atoms in molecules (QTAIM) based on the density functional theory (DFT). The different colors denote different bonding mechanisms, identified by a clear property portfolio for each of these bond types [10]. The fact that these

colors are located in well-defined regions implies that ES and ET are two good quantum-chemical bonding descriptors. Typical PCMs and thermoelectric materials are highlighted in blue and orange rings, respectively, on the map. Interestingly, they both appear in the green area where a bonding mechanism called metavalent bonding prevails. This bonding mechanism deserves a new name, different from classic covalent, ionic, and metallic bonds, because it leads to a unique combination of properties in solids [14, 15]. This portfolio includes an electrical conductivity close to the Mooij rule for bad metals, an effective coordination number that does not satisfy the "8-N " rule for covalent bonds, a large optical dielectric constant that implies the valence electrons are highly polarizable, a high Born effective charge indicative of a high polarizability of chemical bonds, and a large Grüneisen parameter for the transverse optical mode that indicates strong lattice anharmonicity



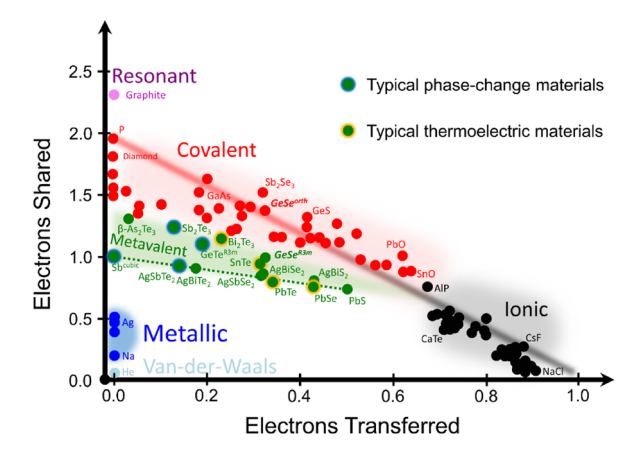


Figure 2: A chemical bonding map spanned by the number of electrons transferred (ET) and electrons shared (ES) between adjacent atoms derived from the quantum theory of molecules in atoms (QTAIM). Typical phase-change materials and thermoelectric materials are highlighted in blue and yellow circles on the map, respectively. Adapted from Refs.

[15, 16]. Solids with different properties have been classified into different groups based on the expectation–maximization algorithm with minimal human interference. The computer-based and expert-based classifications show excellent consistency [10], corroborating that metavalent bonding is indeed a unique bonding mechanism.

In addition, the different types of chemical bonds can be distinguished in a laser-assisted high-field evaporation process, for example, in atom probe tomography (APT) measurements. Figure 3(A) depicts the basic principle of APT [17]. A high positive DC voltage is applied to a needle-shaped specimen to create an intense electric field, typically in the order of tens of V/nm. An ultrashort (10 ps) laser pulse will be used to control the evaporation (i.e., bond-breaking) process. The surface atoms desorb from the bulk and fly toward a position-sensitive detector, where the spatial coordinates and the flight time are recorded. From the flight time, the mass of the ion and hence its chemical identity is determined, while the

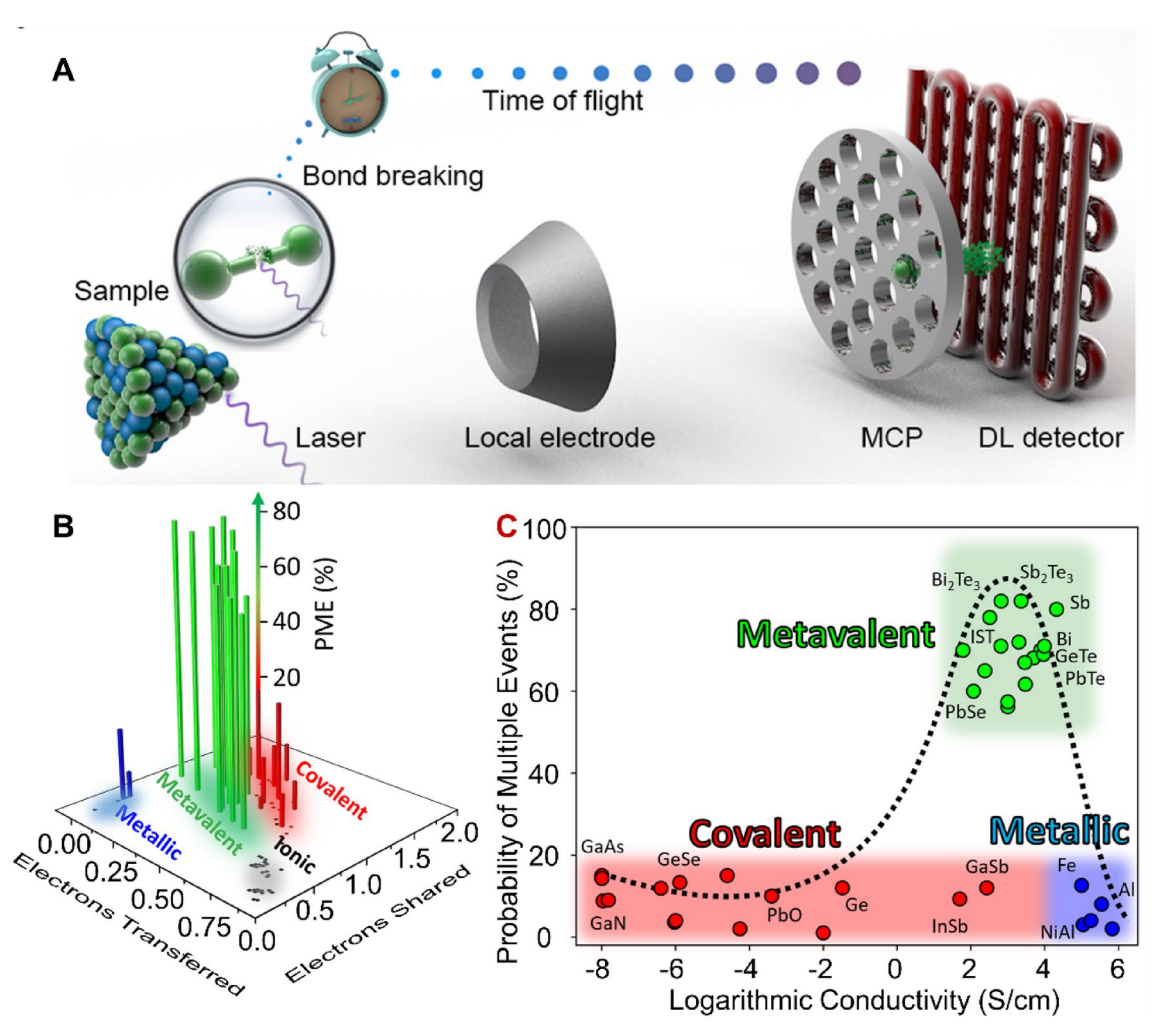


Figure 3: Abnormal bond-rupture of metavalently bonded solids characterized by atom probe tomography (APT). (A) Schematic of APT. Adapted from Ref. 17. (B) The probability of multiple events (PME) plotted on the basal plane of the ES-ET map, highlighting the unique bond-rupture behavior of metavalent bonding. Adapted from Ref. 19. (C) PME versus the electrical conductivity (at room temperature), showing that high PME values can only be observed in the competition zone between electron localization and delocalization. Adapted from Ref. 18.



position of the ion in the sample is derived from the coordinates where the ion hits the detector. The surface atoms can either evaporate in the form of a charged atom or a charged molecule. The probability of producing such molecular ions is called PMI. A successful laser pulse, i.e., a pulse that produces a fragment, usually results in the evaporation of either a single ion or a molecular ion. This process is called a single event. In some cases, a successful laser pulse can also produce the evaporation of two or more separate ions, which is called multiple events. The probability of multiple events is termed PME. PMI and PME can be used to distinguish the bonding mechanisms, as has been explained recently [18, 19]. Fig. 3(B) shows that all metavalently bonded solids exhibit a PME value of larger than 60%, which is strong experimental evidence of a distinct bonding mechanism [19]. Fig. 3(C) further indicates that this abnormal bond-breaking behavior is only observed in the competition zone between the electron delocalization as in metallic bonds and electron localization as in iono-covalent bonds [18]. This transition is found in the conductivity range characterized by the Mooij border for bad metals. Therefore, there is apparently a strong correlation between the peculiar electronic properties of materials and their unconventional bond-breaking behavior.

Design of phase-change materials using metavalent bonding

The capability of data storage in PCMs depends on their large optical and/or electrical contrast between amorphous and crystalline states. As early as 1932, Zachariasen stated that the short-range order in a glass should be the same as in the corresponding crystal since "the atoms are held together by the same forces" [20]. This is true in typical (oxide) glasses, such as SiO_2 . For example, it is (almost) impossible to observe a difference in the optical properties such as reflectance and transmittance between crystalline and amorphous SiO_2 [21]. The same phenomenon also holds for amorphous and crystalline metals. Thus, these classes of materials cannot be used for optical data storage. In striking contrast, the optical reflectance of crystalline PCMs such as $GeSb_2Te_4$ is significantly larger than that of its amorphous counterpart [21]. This different behavior can be understood from a chemical bonding perspective.

Figure 4(A) shows that the ET and ES values hardly differ for crystalline and amorphous SiO₂. [22] This is in line with the statement of Zachariasen that the atomic force (i.e., chemical bonds) are the same in both phases of SiO₂. A similar phenomenon has also been observed for GeSe and GeSe₂. Their amorphous compounds are thus called Zachariasen glasses [22]. On the contrary, crystalline and amorphous PCMs such as GeTe, Sb₂Te₃, and GeSb₂Te₄, show a significant change of bonding upon crystallization. While the crystalline phases are located

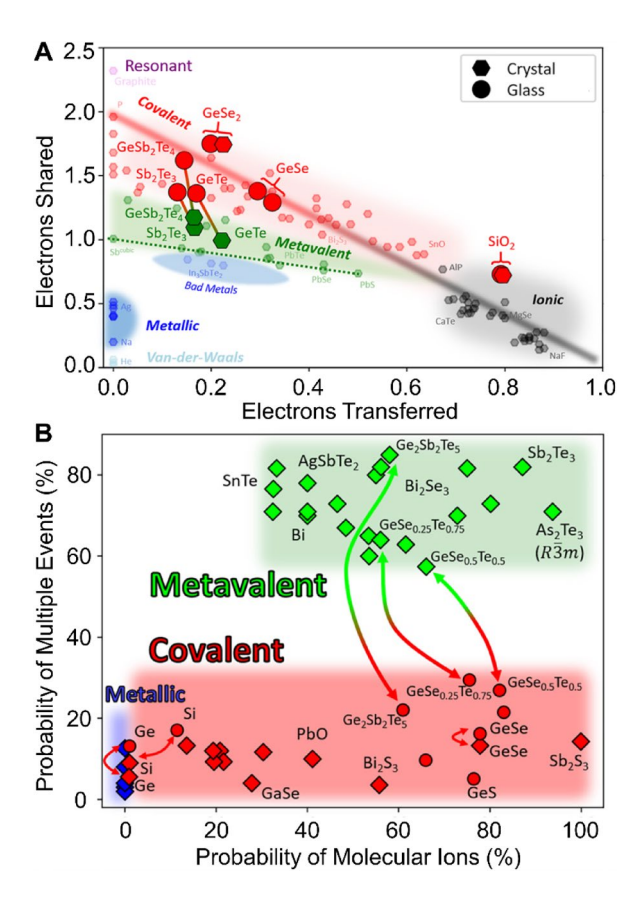


Figure 4: Bonding mechanisms of classic (Zachariasen) and unconventional (non-Zachariasen) glasses and their corresponding crystalline states. (A) The ES-ET map with data for crystals (hexagons) and glasses (circles) of SiO₂, GeSe₂, GeSe, GeTe, Sb₂Te₃, and GeSb₂Te₄, based on Fig. 2. Adapted from Ref. 22. (B) The PMI-PME map, which shows the changes of bonding upon crystallization (arrows). Crystals and glasses are characterized by diamonds and circles, respectively. While classic glasses show negligible changes upon crystallization, amorphous PCMs exhibit pronounced changes in the PME value once they are crystallized. Adapted from Ref. 23.

in the metavalent bonding region, their amorphous counterparts shift to the covalent bonding region. Therefore, amorphous PCMs form non-Zachariasen glasses.

The change in the bonding mechanism upon crystallization can be verified experimentally by measuring the bondbreaking behavior. Figure 4(B) shows the plot of PME versus PMI for many different compounds, where the crystalline state is depicted by diamonds and the amorphous state by circles [23]. No significant differences regarding the PME and PMI values have been observed in Si, Ge, and GeSe between both states. In contrast, PCMs such as $Ge_2Sb_2Te_5$, $GeSe_{0.25}Te_{0.75}$, and $GeSe_{0.5}Te_{0.5}$ show a pronounced increase in the PME upon crystallization. Both the ES-ET map and the APT results thus demonstrate the unique bonding in crystalline PCMs.

Besides the large optical contrast required for data storage and photonic devices, rapid crystallization is another necessity for PCMs. This feature is critical for a universal memory



combining the advantages of DRAM (fast) and Flash (nonvolatile) [24]. Since the RESET process (from crystalline to amorphous) is realized by quenching the liquid phase, which is often very fast (~10 ps) [25], the data processing speed is mainly limited by the SET process, i.e., the crystallization kinetics. The abovementioned Zachariasen glass, e.g., SiO2, shows a very slow crystallization process [26]. In contrast, the phase-change material Ge₂Sb₂Te₅ exhibits a SET speed of about 10–100 ns [27]. This implies that the crystallization kinetics can be manipulated by tailoring the bonding mechanism. The crystallization kinetics are driven either by nucleation or growth. In the nucleationdominated case, crystallization occurs through the stochastic formation of critical nuclei and subsequent growth [28]. Thus, multiple grains with random crystallographic orientations are often observed. On the contrary, in the growth-dominated case, crystallization often starts at the interface of the amorphous region and its surrounding crystalline matrix [28]. Subsequently, the crystallized part grows toward the center of the amorphous region without forming new nuclei. The crystallization speed can be measured by a so-called power-time-effect (PTE) diagram. Figure 5(A) shows that the crystallization time for as-deposited amorphous Ge₂Sb₂Te₅ is about 100 ns. [29] The corresponding electron backscatter diffraction (EBSD) characterization of the crystallized spot [Fig. 5(B)] shows a polycrystalline feature, indicative of a nucleation-driven process. In contrast, the crystallization time increases to 10⁵ ns, and the crystallization process becomes growth-dominated for Ge₂SeTe, as shown in Fig. 5(C) and (D), respectively. Moreover, the slow-nucleation material shows stronger stochasticity, as evidenced by the more scattered data points in Fig. 5(C) at the onset of crystallization. A systematic increase in the minimum nucleation time has been observed in the GeTe-GeSe system by increasing the content of GeSe [30]. In contrast, increasing the content of SnTe in the GeTe-SnTe system decreases the minimum nucleation time, as illustrated in Fig. 5(E). Note that SnTe employs a cubic structure, and GeTe utilizes a rhombohedral structure with a small Peierls distortion, while GeSe is stabilized in an orthorhombic structure with a much larger Peierls distortion. It appears that reducing the degree of Peierls distortion (i.e., decreasing ES) can lower the minimum nucleation time [30]. Thus, the bonding map provides predictive power to tailor the crystallization kinetics of phasechange materials. This is of paramount significance to designing high-speed storage-class memories.

Design of thermoelectric materials using metavalent bonding

Another important application of chalcogenides is thermoelectric energy conversion. Indeed, typical phase-change materials also show decent and even excellent thermoelectric performance [31–34]. As has been summarized in the

thermoelectric figure-of-merit, zT, an excellent thermoelectric performance requires efficient charge transport (high σ) yet inefficient thermal transport (low κ), i.e., an electron crystal and a phonon glass [35]. The electrons in metavalently bonded solids are rather delocalized, leading to a moderately high electrical conductivity (normally between 10 and 10⁴ S/cm). In addition, the small bond order (0.5) leads to soft bonds, while strong interactions between electrons and phonons lead to significant lattice anharmonicity. Both factors result in a low lattice thermal conductivity. Moreover, the rather symmetric crystal structure due to the orthogonal alignment of p-orbitals gives rise to a high valley degeneracy in the reciprocal space, which is beneficial to high Seebeck coefficients. All these attributes are favorable for thermoelectric materials [36]. Therefore, metavalently bonded solids such as Bi₂Te₃, [12] PbTe [37], GeTe [38], and AgSbTe₂ [39] are naturally good thermoelectrics.

However, not all chalcogenides are metavalently bonded. Can they be promising thermoelectric candidates? Does the metavalent bonding theory provide insights into improving the thermoelectric properties of these chalcogenides? Fig. 2 shows that the pristine orthorhombic GeSe utilizes covalent bonding. This results in a very low zT value of less than 0.1 [40]. Conventional doping strategies such as introducing Na, Cu, Ag, As, and iodine could not enhance its zT value significantly [40]. In stark contrast, alloying GeSe with GeTe [41], Sb2Te3 [42], and AgVVI₂ compounds [43-46] could dramatically improve the zT value to near or even above 1.0. APT results demonstrate a distinctive difference in the PME value between pristine GeSe and a GeSe-15%AgSbSe₂ alloy [Fig. 6(A)] [47]. While the former shows a PME value of about 30%, typical for covalent bonding, the latter shows a PME value of about 70%, corroborating the presence of metavalent bonds. Figure 6(B) further illustrates a significant enhancement in zT over the whole temperature range measured upon the transformation of bonding from covalent to metavalent. A similar scenario has also been witnessed in polycrystalline SnSe-AgVVI2 alloys [48]. This highlights the significance of advancing thermoelectrics by crossing the border between covalent and metavalent bonding. Potential interesting phenomena could be expected by crossing the border between metavalent and metallic bonds. This proposal employs the predictive power of the bonding map in Fig. 2.

It is worth noting that the formation of metavalent bonds in a solid normally ensures a decent thermoelectric performance, yet does not necessarily mean that the zT value has already been maximized. The optimization of thermoelectric properties depends on a very precise manipulation of electron and phonon transport, which often involves doping [49]. For charge carrier transport, the electronic states near the Fermi energy level ($E_{\rm F}$) are of utmost importance. Are there clear selection rules for dopants to tune the electronic states near



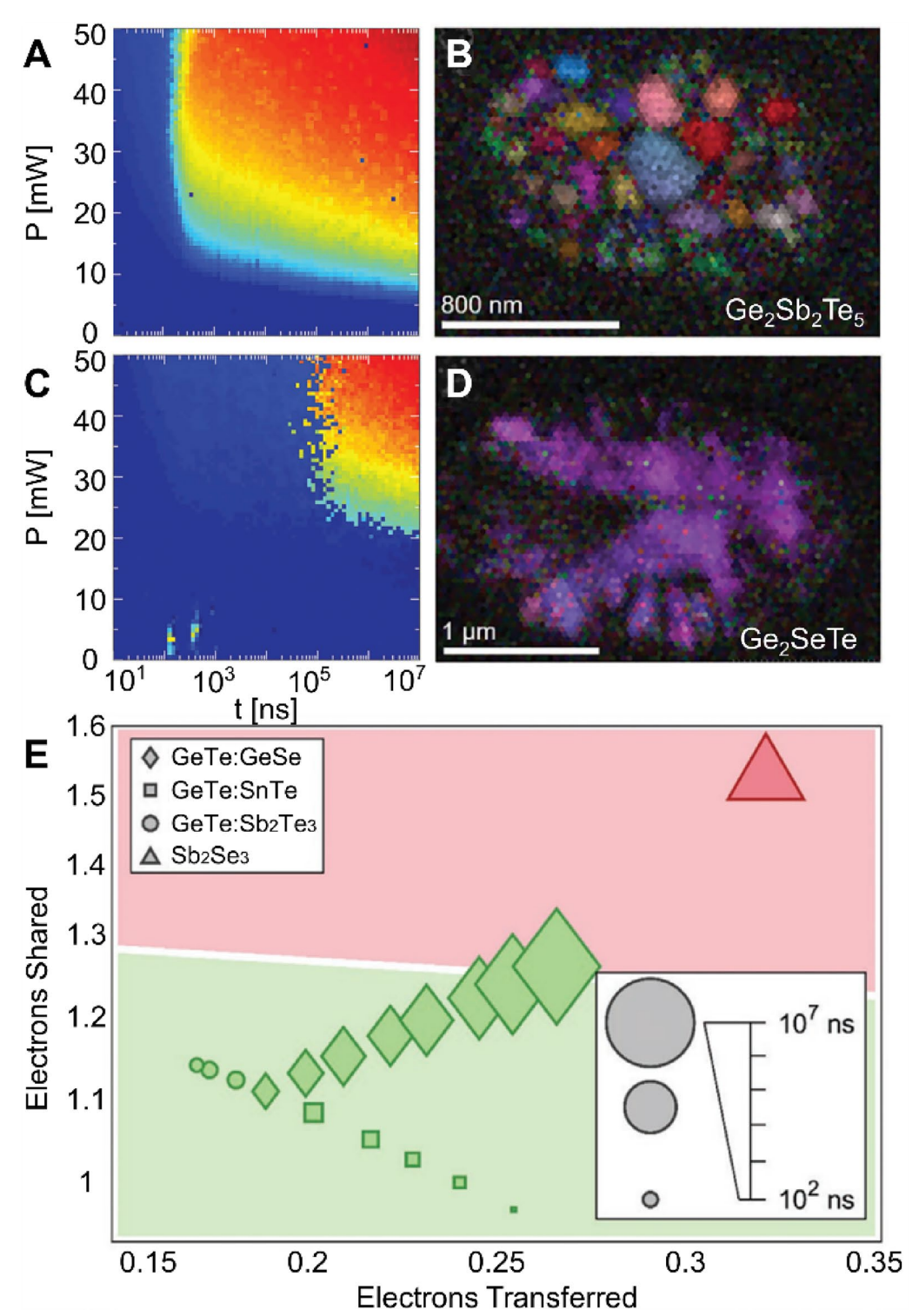


Figure 5: Tuning the crystallization kinetics by engineering chemical bonds. (A) Power-time-effect (PTE) diagram for $Ge_2Sb_2Te_5$. (B) Inverse pole figure overlapped on the image quality map of a crystallized spot in the PTE diagram measured by electron backscatter diffraction (EBSD). (C) PTE diagram for Ge_2SeTe . (D) Corresponding EBSD micrograph of a crystallized spot induced by laser. Adapted from Ref. 29. (E) Dependence of the minimum crystallization time on the ET and ES values. Adapted from Ref. 30.

 E_F ? By combining the perspectives of physics and chemistry, we understand that the cation-s electrons in metavalently bonded solids such as SnTe provide a small (but helpful)

contribution to the electronic states at the L-point of the valence band maximum [50]. The density of states depends on the spatial and energetic overlap between the cation-s and



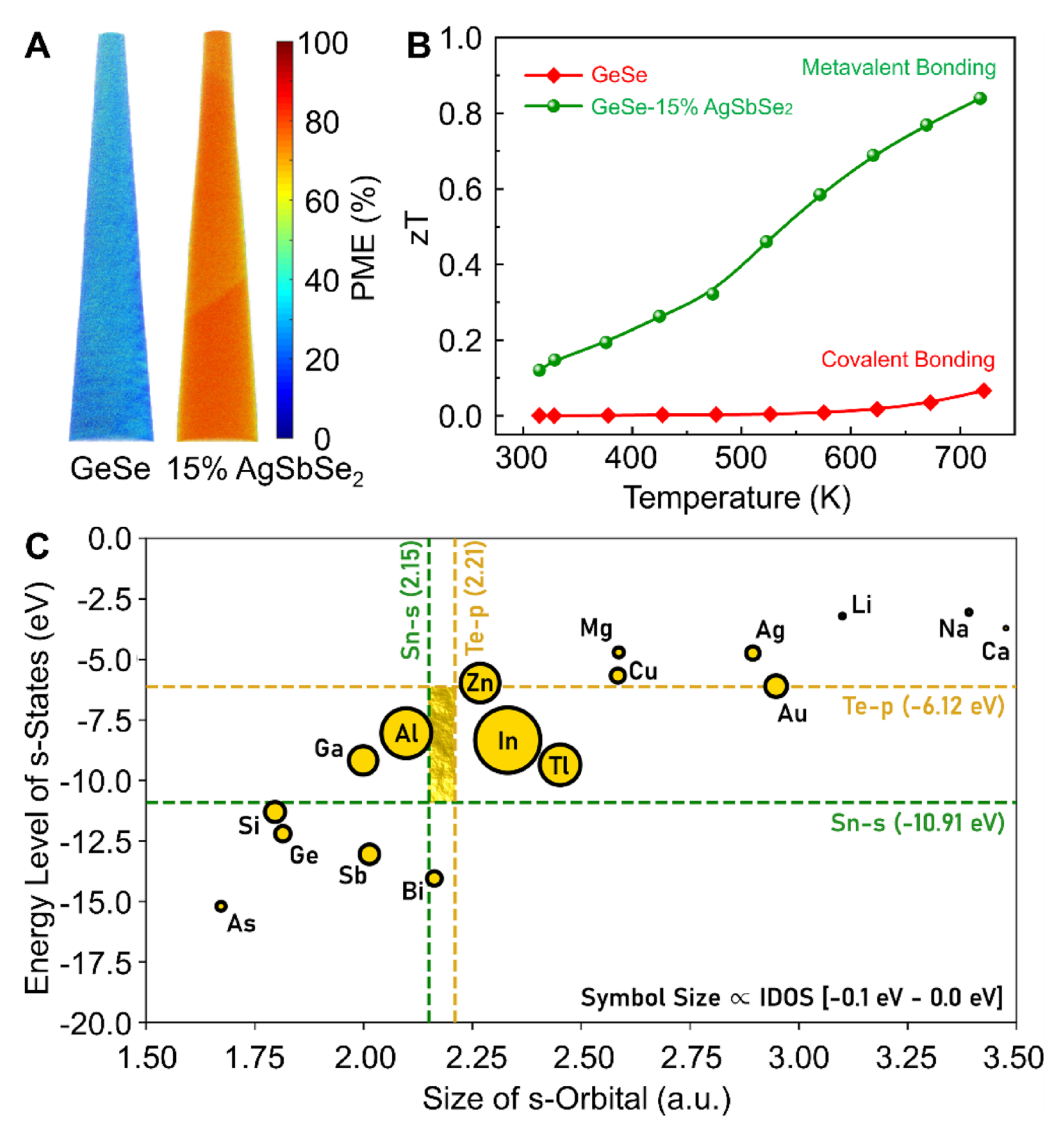


Figure 6: Designing thermoelectrics by tailoring chemical bonds and the interactions between host and dopant orbitals. (A) PME figure for GeSe and GeSe-15%AgSbSe₂ measured by APT. A low PME value (30%) for GeSe indicates its covalent bonding nature. In contrast, a high PME value (~70%) demonstrates metavalent bonding for GeSe-15%AgSbSe₂. (B) Temperature-dependent zT values for covalently bonded GeSe and metavalently bonded GeSe-15%AgSbSe₂ alloy. A significant enhancement of zT upon the formation of metavalent bonds can be observed. Adapted from Ref. 43. (C) Design rule for dopants in terms of spatial and energetic overlap between orbitals. A plot spanned by the size of s-orbitals and the energy level of s-states for dopants. The "golden rectangle" area highlights the "sweet spot" for efficient dopants to create a large DOS 'hump' in SnTe. Adapted from Ref. 46.

anion-p states. Based on this insight, a "golden rectangle" can be established to select dopants, as shown in Fig. 6(C). The closer the dopant on the map to the golden rectangle, the larger the contribution of the cation s-state. This perspective has helped to screen dopants such as In, Al, Tl, and Zn to increase the density of states in SnTe, increasing the Seebeck coefficient and the final zT value.

The concept of metavalent bonding also plays a role in tuning the microstructures and thus the phonon transport. High-frequency phonons are normally scattered by point defects, while mid- to low-frequency phonons are more effectively scattered by boundaries and precipitates [51]. It has been

demonstrated that mixing metavalently bonded solids can form a solid solution in a large composition range [38, 52]. Yet, phase separation is frequently observed upon alloying metavalently bonded solids with covalent or ionic compounds [38, 53, 54]. In this regard, we can design the microstructure to target the selective scattering of phonons.

Conclusion and outlook

The remarkable property portfolio of chalcogenides for thermoelectric and phase-change memory applications is rooted in their unique bonding mechanism, called metavalent bonding. This



review summarized the underlying bonding indicators (Born effective charge, dielectric constant, and Grüneisen parameter, etc.), the bonding descriptors (numbers of electrons shared, ES, and electrons transferred, ET), and the characteristic bondbreaking (probability of molecular ions, PMI, and probability of multiple events, PME) for different chemical bonds. All results support that metavalent bonding is distinctively different from conventional covalent, ionic, and metallic bonding. Understanding this bonding mechanism has enabled the design of the nucleation and crystallization kinetics of phase-change materials, as well as the electron and phonon transport of thermoelectric materials. The two bonding descriptors, i.e., ES and ET, can be considered excellent property predictors. Combined with the advanced calculation and characterization tools, tailoring metavalent bonds is expected to bring a new era for next-generation phase-change and thermoelectric materials and to explore uncharted territory for more applications of chalcogenides.

Author contributions

Y.Y and M.W conceived this work. Y.Y wrote the manuscript. M.W edited the manuscript.

Funding

Open Access funding enabled and organized by Projekt DEAL. This work is financially supported by the Deutsche Forschungsgemeinschaft (DFG) via the collaborative research center Nanoswitches (SFB 917).

Data availability

Not applicable.

Declarations

Competing interests The authors declare that they have no competing interests.

Open Access

This article is licensed under a Creative Commons Attribution 4.0 International License, which permits use, sharing, adaptation, distribution and reproduction in any medium or format, as long as you give appropriate credit to the original author(s) and the source, provide a link to the Creative Commons licence, and indicate if changes were made. The images or other third party material in this article are included in the article's Creative Commons licence, unless indicated otherwise in a credit line to the material. If material is not included in the article's Creative Commons licence and your intended use is not permitted by statutory regulation or exceeds the permitted use, you will need to obtain permission directly from the copyright

holder. To view a copy of this licence, visit http://creativecommons.org/licenses/by/4.0/.

References

- W. Zhang, E. Ma, Unveiling the structural origin to control resistance drift in phase-change memory materials. Mater. Today 41, 156 (2020)
- X.-L. Shi, J. Zou, Z.-G. Chen, Advanced thermoelectric design: from materials and structures to devices. Chem. Rev. 120(15), 7399 (2020)
- 3. M. Wuttig, N. Yamada, Phase-change materials for rewriteable data storage. Nat. Mater. **6**(11), 824 (2007)
- J. He, T.M. Tritt, Advances in thermoelectric materials research: looking back and moving forward. Science 357(6358), e9997 (2017)
- D. Lencer, M. Salinga, B. Grabowski, T. Hickel, J. Neugebauer, M. Wuttig, A map for phase-change materials. Nat. Mater. 7(12), 972 (2008)
- M. Hong, M. Li, Y. Wang, X.-L. Shi, Z.-G. Chen, Advances in versatile GeTe thermoelectrics from materials to devices. Adv. Mater. 35(2), 2208272 (2023)
- Y. Yu, D.-S. He, S. Zhang, O. Cojocaru-Mirédin, T. Schwarz, A. Stoffers, X.-Y. Wang, S. Zheng, B. Zhu, C. Scheu, D. Wu, J.-Q. He, M. Wuttig, Z.-Y. Huang, F.-Q. Zu, Simultaneous optimization of electrical and thermal transport properties of Bi 0.5 Sb 1.5
 Te 3 thermoelectric alloy by twin boundary engineering. Nano Energy 37, 203 (2017)
- 8. Y. Xiao, L.-D. Zhao, Charge and phonon transport in PbTe-based thermoelectric materials. npj Quant. Mater. **3**(1), 55 (2018)
- 9. L. Li, B. Hu, Q. Liu, X.-L. Shi, Z.-G. Chen, High-performance AgSbTe2 thermoelectrics: advances, challenges, and perspectives. Adv. Mater. **36**(45), 2409275 (2024)
- C.-F. Schön, S. van Bergerem, C. Mattes, A. Yadav, M. Grohe, L. Kobbelt, M. Wuttig, Classification of properties and their relation to chemical bonding: essential steps toward the inverse design of functional materials. Sci. Adv. 8(47), e0828 (2022)
- J.Y. Raty, M. Schumacher, P. Golub, V.L. Deringer, C. Gatti, M.
 Wuttig, A quantum-mechanical map for bonding and properties in solids. Adv. Mater. 31(3), 1806280 (2019)
- 12. Y. Cheng, O. Cojocaru-Miredin, J. Keutgen, Y. Yu, M. Kupers, M. Schumacher, P. Golub, J.Y. Raty, R. Dronskowski, M. Wuttig, Understanding the structure and properties of sesqui-chalcogenides (i.e., V2 VI3 or Pn2 Ch3 (Pn = Pnictogen, Ch = Chalcogen) compounds) from a bonding perspective. Adv. Mater. 31(43), 1904316 (2019)
- M. Wuttig, C.-F. Schön, J. Lötfering, P. Golub, C. Gatti, J.-Y. Raty, Revisiting the nature of chemical bonding in chalcogenides to explain and design their properties. Adv. Mater. 35(20), 2208485 (2022)



- R. Arora, U.V. Waghmare, C.N.R. Rao, Metavalent bonding origins of unusual properties of group IV chalcogenides. Adv. Mater. 35(7), 2208724 (2022)
- M. Wuttig, V.L. Deringer, X. Gonze, C. Bichara, J.Y. Raty, Incipient metals: functional materials with a unique bonding mechanism. Adv. Mater. 30(51), 1803777 (2018)
- B.J. Kooi, M. Wuttig, Chalcogenides by design: functionality through metavalent bonding and confinement. Adv. Mater. 32(21), 1908302 (2020)
- 17. Y. Yu, C. Zhou, S. Zhang, M. Zhu, M. Wuttig, C. Scheu, D. Raabe, G.J. Snyder, B. Gault, O. Cojocaru-Mirédin, Revealing nano-chemistry at lattice defects in thermoelectric materials using atom probe tomography. Mater. Today 32, 260 (2020)
- O. Cojocaru-Miredin, Y. Yu, J. Kottgen, T. Ghosh, C.F. Schon, S. Han, C. Zhou, M. Zhu, M. Wuttig, Atom probe tomography: a local probe for chemical bonds in solids. Adv. Mater. 36(50), 2403046 (2024)
- Y. Yu, O. Cojocaru-Mirédin, M. Wuttig, Atom probe tomography advances chalcogenide phase-change and thermoelectric materials. Phys. Status Solidi A 221(22), 2300425 (2024)
- W.H. Zachariasen, The atomic arrangement in glass. J. Am. Chem. Soc. 54(10), 3841 (1932)
- M. Wuttig, Phase change materials: chalcogenides with remarkable properties due to an unconventional bonding mechanism. Phys. Status Solidi (b). 249(10), 1843 (2012)
- J.-Y. Raty, C. Bichara, C.-F. Schön, C. Gatti, M. Wuttig, Tailoring chemical bonds to design unconventional glasses. Proceed. Nat. Acad. Sci. 121(2), e2316498121 (2024)
- J.-Y. Raty, C. Bichara, C.-F. Schön, C. Gatti, M. Wuttig, Reply to Lee and Elliott: changes of bonding upon crystallization in phase change materials. Proceed. Nat. Acad. Sci. 121(19), e2405294121 (2024)
- 24. W. Zhang, R. Mazzarello, E. Ma, Phase-change materials in electronics and photonics. MRS Bull. **44**(9), 686 (2019)
- B. Wu, T. Wei, Q. Liu, Y. Cheng, Y. Zheng, R. Wang, Q. Liu, M. Cheng, W. Li, J. Hu, Y. Ling, B. Liu, Ultrafast SET/RESET operation for optoelectronic hybrid phase-change memory device cells based on Ge2Sb2Te5 material using partial crystallization strategy. Appl. Phys. Lett. 123(19), 191110 (2023)
- R.S. Hay, Crystallization kinetics for SiO2 formed during SiC fiber oxidation in steam. J. Am. Ceram. Soc. 102(9), 5587 (2019)
- M. Lanza, A. Sebastian, W.D. Lu, M. Le Gallo, M.-F. Chang, D. Akinwande, F.M. Puglisi, H.N. Alshareef, M. Liu, J.B. Roldan, Memristive technologies for data storage, computation, encryption, and radio-frequency communication. Science 376(6597), eabi9979 (2022)
- W. Zhang, R. Mazzarello, M. Wuttig, E. Ma, Designing crystallization in phase-change materials for universal memory and neuro-inspired computing. Nat. Rev. Mater. (2019). https://doi. org/10.1038/s41578-018-0076-x

- M.J. Müller, C. Morell, P. Kerres, M. Raghuwanshi, R. Pfeiffer, S. Meyer, C. Stenz, J. Wang, D.N. Chigrin, P. Lucas, M. Wuttig, Decoupling nucleation and growth in fast crystallization of phase change. Mater. Adv. Funct. Mater. 34(39), 2403476 (2024)
- C. Persch, M.J. Muller, A. Yadav, J. Pries, N. Honne, P. Kerres,
 S. Wei, H. Tanaka, P. Fantini, E. Varesi, F. Pellizzer, M. Wuttig,
 The potential of chemical bonding to design crystallization and vitrification kinetics. Nat. Commun. 12(1), 4978 (2021)
- M.N. Schneider, T. Rosenthal, C. Stiewe, O. Oeckler, From phasechange materials to thermoelectrics? Z. Kristallogr. 225(11), 463 (2010)
- 32. Y. Jiang, T.-R. Wei, X. Shi, Beyond phase-change materials: Pseudo-binary (GeTe)n(Sb2Te3)m alloys as promising thermoelectric materials. Mater. Today Phys. **36**, 101167 (2023)
- P. Hu, T.R. Wei, P. Qiu, Y. Cao, J. Yang, X. Shi, L. Chen, Largely enhanced seebeck coefficient and thermoelectric performance by the distortion of electronic density of states in Ge2Sb2Te5. ACS Appl. Mater. Interfaces 11(37), 34046 (2019)
- E.-R. Sittner, K.S. Siegert, P. Jost, C. Schlockermann, F.R.L. Lange, M. Wuttig, (GeTe)x-(Sb2Te3)1-xphase-change thin films as potential thermoelectric materials. Phys. Status Solidi A 210(1), 147 (2013)
- T. Zhu, Y. Liu, C. Fu, J.P. Heremans, G.J. Snyder, X. Zhao, Compromise and synergy in high-efficiency thermoelectric materials. Adv. Mater. 29(14), 1605884 (2017)
- Y. Yu, M. Cagnoni, O. Cojocaru-Mirédin, M. Wuttig, Chalcogenide thermoelectrics empowered by an unconventional bonding mechanism. Adv. Funct. Mater. 30(8), 1904862 (2020)
- R. Wu, Y. Yu, S. Jia, C. Zhou, O. Cojocaru-Miredin, M. Wuttig, Strong charge carrier scattering at grain boundaries of PbTe caused by the collapse of metavalent bonding. Nat. Commun. 14(1), 719 (2023)
- M. Liu, M. Guo, H. Lyu, Y. Lai, Y. Zhu, F. Guo, Y. Yang, K. Yu, X. Dong, Z. Liu, W. Cai, M. Wuttig, Y. Yu, J. Sui, Doping strategy in metavalently bonded materials for advancing thermoelectric performance. Nat. Commun. 15(1), 8286 (2024)
- Y. Wu, P. Qiu, Y. Yu, Y. Xiong, T. Deng, O. Cojocaru-Mirédin, M. Wuttig, X. Shi, L. Chen, High-performance and stable AgSbTe2based thermoelectric materials for near room temperature applications. J. Mater. 8(6), 1095 (2022)
- 40. X. Zhang, J. Shen, S. Lin, J. Li, Z. Chen, W. Li, Y. Pei, Thermoelectric properties of GeSe. J. Mater. 2(4), 331 (2016)
- J. Cui, C. Xie, W. Hu, H. Luo, Q. Mei, S. Li, W. Xu, Z. Gao, J. Wu, Q. Zhang, X. Tang, G. Tan, Two-dimensional-like phonons in three-dimensional-structured rhombohedral GeSe-based compounds with excellent thermoelectric performance. ACS Appl. Mater. Interfaces 16(30), 39656 (2024)
- 42. H. Luo, X.-L. Shi, Y. Liu, M. Li, M. Zhang, X. Luo, M. Wang, X. Huang, L. Hu, Z.-G. Chen, Metavalent alloying and vacancy engineering enable state-of-the-art cubic GeSe thermoelectrics. Nat. Commun. **16**(1), 3136 (2025)



- M. Zhang, X.-L. Shi, Y. Mao, M. Li, R. Moshwan, T. Cao, W. Chen, L. Yin, W. Lyu, Y. Chen, S. Liu, W.-D. Liu, Q. Liu, G. Tang, Z.-G. Chen, High-performance GeSe-based thermoelectrics via Cu-doping. Adv. Funct. Mater. 34(52), 2411054 (2024)
- D. Sarkar, T. Ghosh, S. Roychowdhury, R. Arora, S. Sajan, G. Sheet, U.V. Waghmare, K. Biswas, Ferroelectric instability induced ultralow thermal conductivity and high thermoelectric performance in rhombohedral p-type GeSe crystal. J. Am. Chem. Soc. 142(28), 12237 (2020)
- D. Sarkar, S. Roychowdhury, R. Arora, T. Ghosh, A. Vasdev, B. Joseph, G. Sheet, U.V. Waghmare, K. Biswas, Metavalent bonding in GeSe leads to high thermoelectric performance. Angew. Chem. Int. Ed. Engl. 60(18), 10350 (2021)
- T. Lyu, M. Wang, X. Luo, Y. Zhou, L. Chen, M. Hong, L. Hu, Advanced GeSe-based thermoelectric materials: progress and future challenge. Appl. Phys. Rev. 11(3), 031323 (2024)
- Y. Yu, C. Zhou, T. Ghosh, C.F. Schon, Y. Zhou, S. Wahl, M. Raghuwanshi, P. Kerres, C. Bellin, A. Shukla, O. Cojocaru-Miredin, M. Wuttig, Doping by design: enhanced thermoelectric performance of GeSe alloys through metavalent bonding. Adv. Mater. 35(19), 2300893 (2023)
- N. Lin, S. Han, T. Ghosh, C.F. Schön, D. Kim, J. Frank, F. Hoff, T. Schmidt, P. Ying, Y. Zhu, M. Häser, M. Shen, M. Liu, J. Sui, O. Cojocaru-Mirédin, C. Zhou, R. He, M. Wuttig, Y. Yu, Metavalent bonding in cubic SnSe alloys improves thermoelectric properties over a broad temperature range. Adv. Funct. Mater. 34(30), 2315652 (2024)
- Q. Xiong, G. Han, G. Wang, X. Lu, X. Zhou, The doping strategies for modulation of transport properties in thermoelectric. Mater. Adv. Funct. Mater. 34(52), 2411304 (2024)

- 50. G. Tang, Y. Liu, X. Yang, Y. Zhang, P. Nan, P. Ying, Y. Gong, X. Zhang, B. Ge, N. Lin, X. Miao, K. Song, C.F. Schon, M. Cagnoni, D. Kim, Y. Yu, M. Wuttig, Interplay between metavalent bonds and dopant orbitals enables the design of SnTe thermoelectrics. Nat. Commun. 15(1), 9133 (2024)
- 51. H. Kim, G. Park, S. Park, W. Kim, Strategies for manipulating phonon transport in solids. ACS Nano 15(2), 2182 (2021)
- Y. Liu, X. Zhang, P. Nan, B. Zou, Q. Zhang, Y. Hou, S. Li, Y. Gong, Q. Liu, B. Ge, O. Cojocaru-Mirédin, Y. Yu, Y. Zhang, G. Chen, M. Wuttig, G. Tang, Improved solubility in metavalently bonded solid leads to band alignment, ultralow thermal conductivity, and high thermoelectric performance in SnTe. Adv. Funct. Mater. 220, 9980 (2022)
- 53. D. An, J. Wang, J. Zhang, X. Zhai, Z. Kang, W. Fan, J. Yan, Y. Liu, L. Lu, C.-L. Jia, M. Wuttig, O. Cojocaru-Mirédin, S. Chen, W. Wang, G.J. Snyder, Y. Yu, Retarding Ostwald ripening through Gibbs adsorption and interfacial complexions leads to high-performance SnTe thermoelectrics. Energy Environ. Sci. 14(10), 5469 (2021)
- 54. Y. Yu, A. Sheskin, Z. Wang, A. Uzhansky, Y. Natanzon, M. Dawod, L. Abdellaoui, T. Schwarz, C. Scheu, M. Wuttig, O. Cojocaru-Mirédin, Y. Amouyal, S. Zhang, Ostwald ripening of Ag2Te precipitates in thermoelectric PbTe: effects of crystallography, dislocations, and interatomic bonding. Adv. Energy Mater. 14(19), 2304442 (2024)

Publisher's Note Springer Nature remains neutral with regard to jurisdictional claims in published maps and institutional affiliations.